J. Wind Eng. Ind. Aerodyn. 126 (2014) 1–10

Contents lists available at ScienceDirect

Journal of Wind Engineering and Industrial Aerodynamics

journal homepage: www.elsevier.com/locate/jweia

Effect of air density on the performance of a small wind turbine blade: A case study in Iran

Abolfazl Pourrajabian [a,*], Masoud Mirzaei [a], Reza Ebrahimi [a], David Wood [b]

[a] Faculty of Aerospace Engineering, K.N. Toosi University of Technology, 16765-3381 Tehran, Iran
[b] Department of Mechanical and Manufacturing Engineering, University of Calgary, Calgary, T2N 1N4, Canada

ARTICLE INFO

Article history:
Received 15 September 2013
Received in revised form
1 January 2014
Accepted 1 January 2014
Available online 25 January 2014

Keywords:
Small wind turbine
Air density
Iran
Altitude
Blade
Staring time
Optimization
Genetic algorithm

ABSTRACT

The influence of the air density variation with altitude on the performance of a small horizontal axis wind turbine blade was studied for four regions of good wind resources in Iran and altitudes up to 3000 m. In order to improve the performance of the turbine at low wind speed, starting time was combined with output power in an objective function and a three-bladed, 2 m diameter rotor was designed and optimized for those regions using a purpose-built genetic algorithm. The Blade-Element Momentum (BEM) theory was employed to calculate the output power and a modified version was used to determine the starting time in the presence of a small, but significant resistive torque. The optimization procedure maximized a combination of the output power in terms of the power coefficient and the starting time. Results show that the performance of a blade optimized for sea level degrades for other locations and that degradation is more important for the starting performance than the power coefficient. In order to improve the performance of the blade at the different altitudes, the optimization process was performed in two steps. First, the geometry of the blade was optimized for the air density at the appropriate altitude that increased both the power coefficient and the starting time. Much more power was achieved using the second step in which the tip speed ratio was optimized along with the geometry of the blade in the optimization procedure. The results highlight the importance of the drive train and generator resistive torque which delays the starting of the wind turbine especially at very high altitudes as the aerodynamic torque is reduced.

1. Introduction

Small Wind Turbines (SWTs) have an effective role to supply the increasing demand for the production of electricity especially for remote applications which are often in mountains. According to International Electrotechnical Commission (IEC) Standard 61400-2, IEC (2006), which only considers horizontal-axis turbines, a SWT has a swept area of less than 200 m^2, which corresponds to a power output of about 50 kW. SWTs must be installed close to the load they supply even if the wind resource is poor. There is usually no pitch adjustment on the blades of SWTs because it is too expensive. The absence of pitch adjustment requires advanced blade design to generate lift at high angles of attack during the starting to overcome the resistive torque of the drive train and generator. SWTs blades should also have a high aerodynamic efficiency during the operation to harness the wind energy as much as possible. So, design and optimization of the blades for SWTs is a challenging task and it has a vital role in the overall system design and optimization of the SWTs.

After selection of an airfoil profile, blade optimization has traditionally aimed to find the distributions of the chord and twist to maximize the output power. In the absence of drag and tip losses, the ideal distribution of the chord (c) and twist (θ_p) was determined by Burton et al. (2011) for a chosen airfoil profile with lift coefficient C_l, Tip Speed Ratio (TSR) λ, and number of blades N, as

$$cC_l = \frac{16\pi}{9N\lambda\sqrt{4/9+[\lambda_r+(2/(9\lambda_r))]^2}} \tag{1.1}$$

$$\theta_p = \phi - \alpha, \quad \tan\phi = \frac{2}{3\lambda_r+(2/\lambda_r)} \tag{1.2}$$

where θ_p is the blade pitch (twist) angle (between the chord line and the plane of rotation), α is the angle of attack and the inflow angle (ϕ) can be determined by knowing the local speed ratio, $\lambda_r=(r/R)\lambda$, where R is the tip radius. These ideal equations neglect tip losses which typically affect the optimum values only in the tip region, Clifton-Smith (2009).

Generally, the main goal of design and optimization of a wind turbine blade is to maximize the output power. However, other goals

* Corresponding author. Tel.: +98 9133924107.
E-mail address: abolfazlp915@yahoo.com (A. Pourrajabian).

0167-6105/$ - see front matter © 2014 Elsevier Ltd. All rights reserved.
http://dx.doi.org/10.1016/j.jweia.2014.01.001

must sometimes be considered during the optimization procedure. Mass minimization of the blade to reduce cost, and reduction of noise are other important goals which may be included in the objective function, particularly for large turbines. Starting time is another parameter which must be minimized to improve low wind speed performance of SWTs. Even though the influence of the starting time is unimportant for large wind turbines, it is critical for the low wind speed performance of SWT blades with no pitch adjustment (Ebert and Wood, 1997; Mayer et al., 2001; Wood and Robotham, 1999; Wright and Wood, 2004).

An experiment on a two-bladed 5 kW turbine by Ebert and Wood (1997) revealed two main phases in the starting sequence, namely the initial period of idling followed by one of the rapid acceleration. During the former, the turbine blades rotate with low acceleration and the angle of attack gradually decreases until the blade can generate a high lift to drag ratio. After that, the turbine accelerates rapidly to the point at which useful power can be extracted. Since the rapid acceleration period is comparatively short, it can be neglected in designing a small turbine for improved starting performance. The starting of a three-bladed, 2 m diameter small HAWT was investigated by Wright and Wood (2004). Their results showed that the torque generated near the hub is large during starting while the torque near the tip dominates during power production. They also showed that a simple modification of the blade element theory provided a surprisingly accurate description of starting. The modifications comprised of neglecting axial and circumferential induction, and the use of generic equations for lift and drag at high angles of incidence. Mayer et al. (2001) investigated the effect of collective blade pitch angle on the idling period. They found that increasing the collective pitch caused more rapid starting and the idling period was shortened due to the lower angles of attack. Moreover, they suggested that the collective pitch angle that gives the best starting behavior was 20°.

The above mentioned experimental research led to the design of improved blades having good starting performance and suitable output power. Reducing the moment of inertia and using an evolutionary algorithm, Hampsey (2002) designed an improved turbine blade which could accelerate more quickly with good output power. Later studies by Wood (2004) and Clifton-Smith and Wood (2007) showed that new designs provide a good compromise between the starting torque and the power extraction. Their starting calculations assumed that the difference between the aerodynamic torque and the resistive torque in the drive train accelerated the rotor without extracting power. The resistive torque is dominated by the cogging torque if a permanent magnet generator and no gearbox is used. Alternatively, there will be a frictional torque in a gearbox in combination with an induction generator (Wood, 2011).

One valuable lesson of these multi-dimensional analyses is that the best power-extracting blades always have poor starting performance. However, a large decrease in the starting time could be achieved for a small reduction in output power. Clifton-Smith (2010) considered a sound power level as another parameter in the multi-dimensional analysis. Using Differential Evolution (DE) for optimization, he found a range of blades which limit noise and reduce starting time while retaining power producing performance. It must be emphasized that multi-dimensional optimization uses computationally cheap objective functions to limit as much as possible the parameter range of the final blade design. However, it is not the totality of the blade design. Candidate optimal blades must be analyzed structurally using finite element analysis and their aero-elastic and aerodynamic damping behavior analyzed thoroughly by more complex computational fluid dynamics methods before they are actually made. This combination of multi-objective optimization followed by more detailed design has worked satisfactorily for several previous blades that were manufactured and field tested. The closest example to the blade considered here is the 2.5 m long blade described in Wood (2011) which is currently under extensive field testing at the University of Newcastle, Australia. The experiments include an instrumented blade to determine the actual blade loadings for further study of the aero-elastic behavior of SWT blades. For convenience, the multi-objective optimization used here will be called “design” but the need for subsequent substantial assessment and possible modification is taken as understood.

The main aim of this paper is to investigate the impact of altitude on the performance of a SWT blade. Altitude should have a very predictable influence on power extraction through its effect on the density and kinematic viscosity and, hence, Reynolds number. However, altitude effects on starting are less obvious. We assume that the resistive torque is independent of altitude and so, the reduction in aerodynamic torque with density makes starting progressively more difficult as altitude increases. While the efficiency of power extraction of the SWT is the first objective of the present study, the starting improvement of the SWT is also addressed as another goal and priority. Four sites in Iran of altitudes up to 3000 m are selected as test cases, and a three-bladed, 2 m diameter small HAWT is designed and optimized for those regions. A combination of the starting time and the output power is included in the objective function and a genetic algorithm is used to design a blade for high output power and low starting time.

2. Wind resources in Iran

Situated in the south-western part of Asia, Iran (Persia) is bordered on the north by Armenia, Azerbaijan and Turkmenistan as well as the Caspian Sea, Turkey and Iraq to the west, the Persian Gulf and the Sea of Oman to the south, and Pakistan and Afghanistan to the east (Fig. 1). Persians were pioneers in designing and using windmills for both grinding grain and pumping water. Although the potential capacity of wind energy is high, there is only 91 MW installed capacity by 2012 (Mostafaeipour et al., 2014). Obviously, much more work is still needed to use the available wind power in Iran. Wind energy potential has been assessed for some locations in Iran such as Tehran (Keyhani et al., 2010), Manjil (Mostafaeipour and Abarghooei, 2008) and Shahrbabak (Mostafaeipour et al., 2011). Moreover, the feasibility of offshore wind turbines both in the Caspian Sea and the Persian Gulf has been assessed by Mostafaeipour (2010). There are some excellent regions such as Manjil and Binalud in which the two wind farms have been installed. In order to investigate the effect of altitude on the performance of SWTs, four locations with different altitude were selected, Table 1. The average wind speed of the locations was measured at a height of 30 m. The priority of Renewable Energy Organization of Iran[1] is to harness the wind energy in these, as well as other windy regions. Fig. 2 shows the chosen locations in the wind atlas of Iran. The properties of air on those regions were determined on the basis of International Standard Atmosphere (ISA) (U.S. Standard Atmosphere, 1962).

3. Aerodynamic modeling

The aerodynamic model used here is the Blade-Element Momentum (BEM) theory which is a combination of the momentum and blade element theory. In BEM, the blade is divided into several stations and at each station, the blade element theory is employed to calculate the thrust and torque over the blade element (airfoil) such that the momentum and angular

[1] http://www.suna.org.ir (accessed 02.05.13).

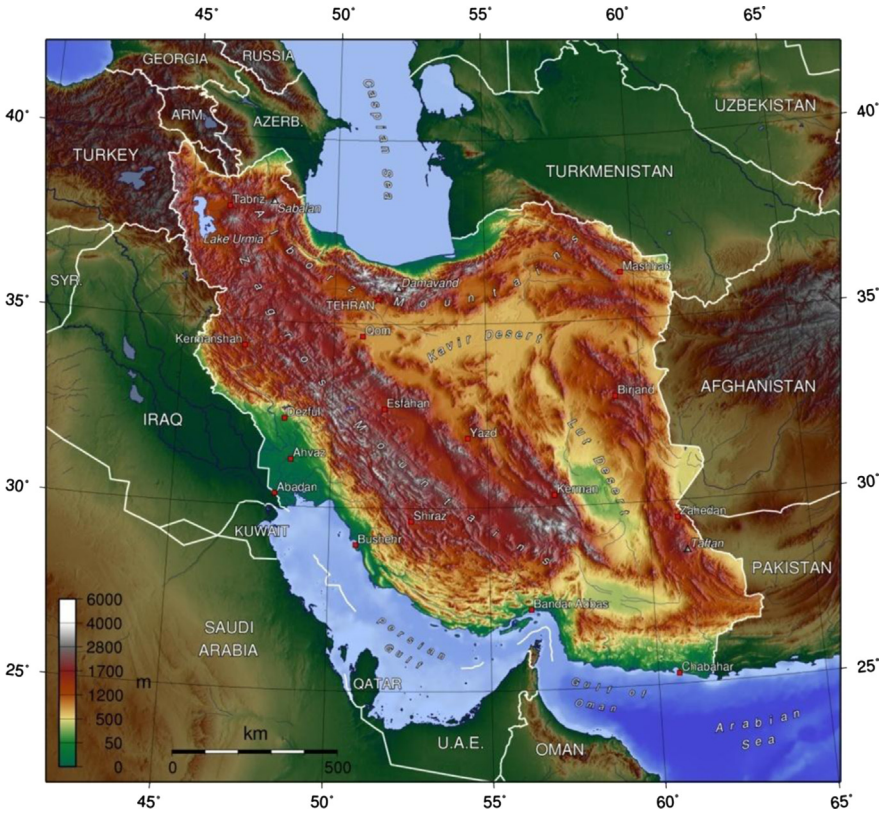

Fig. 1. Topographic map of Iran (Renewable Energy Organization of Iran).

Table 1
Specifications of the considered locations (Renewable Energy Organization of Iran).

Case study	Station name	Coordinates E–N	Height (m)	Air density (kg/m^3)	Average wind speed (m/s)
Sea level	–	–	0	1.225	5
A	Zahak	61°41′–30°54′	495	1.1678	6.1
B	Khoor_birjand	58°26′–32°56′	1117	1.0989	5.8
C	Bijar	47°37′–35°53′	1883.4	1.0183	5.2
D	Firouzkooh_poll	52°24′–35°43′	2985.5	0.9105	5

momentum fluxes in the flow over that blade element balance the thrust and torque. Once the aerodynamic torque (Q) was calculated for the whole blade, the power coefficient and actual power (P) are determined from

$$C_P = \frac{P}{0.5\rho AU^3} = \frac{Q\Omega}{0.5\rho AU^3} \tag{3.1}$$

where A is the swept area of blades, Ω is the angular velocity and U is the wind velocity. Here, a modified version of the BEM theory was used which was identical to that described in Wood (2011). A modified BEM is required to guarantee the accuracy of the computations especially at the blade tip where the losses are important. Tip losses could change the ideal distributions of the chord and twist determined by Eqs. (1.1) and (1.2), but the change is unlikely to be large, (Clifton-Smith, 2009). Prandtl′s tip loss factor relates the wind speed at the blade element to the average wind speed in the annular stream tube flowing over the blade element which is used in the momentum balance. After manipulating the momentum and the blade element equations, Prandtl′s tip loss correction factor, F, which is always less than unity, was applied directly to the momentum and blade element equations as follows

$$F = 2\cos^{-1}(e^{-f})/\pi \tag{3.2}$$

where

$$f = N(R-r)/(2r\ \sin\ \varphi) \tag{3.3}$$

Because of its high lift-to-drag ratio, the SG6043 airfoil was selected for all blades. The SG6043 airfoil was designed by Giguere and Selig (1998) exclusively for SWTs. Its thickness and camber are 10% and 5.5% respectively and it has a large lift-to-drag ratio at $Re = 2.2 \times 10^5$. For this Reynolds number, C_l at maximum lift-to-drag is 1.22 at $\alpha = 5°$. It is common for small blades to use the same airfoil section over the whole blade largely because thick sections, as used in the hub region of large blades, perform badly at low Re. During the analysis of power output, the aerodynamics coefficients at each α and Re were interpolated from a data file constructed from the experimental data taken from Professor Selig′s web site.[2] Since the airfoil of the blade is known at each section, the problem is to find the distribution of the chord and twist to achieve the multiple objectives of the blade design.

[2] http://aerospace.illinois.edu/m-selig/ (accessed 22.05.13).

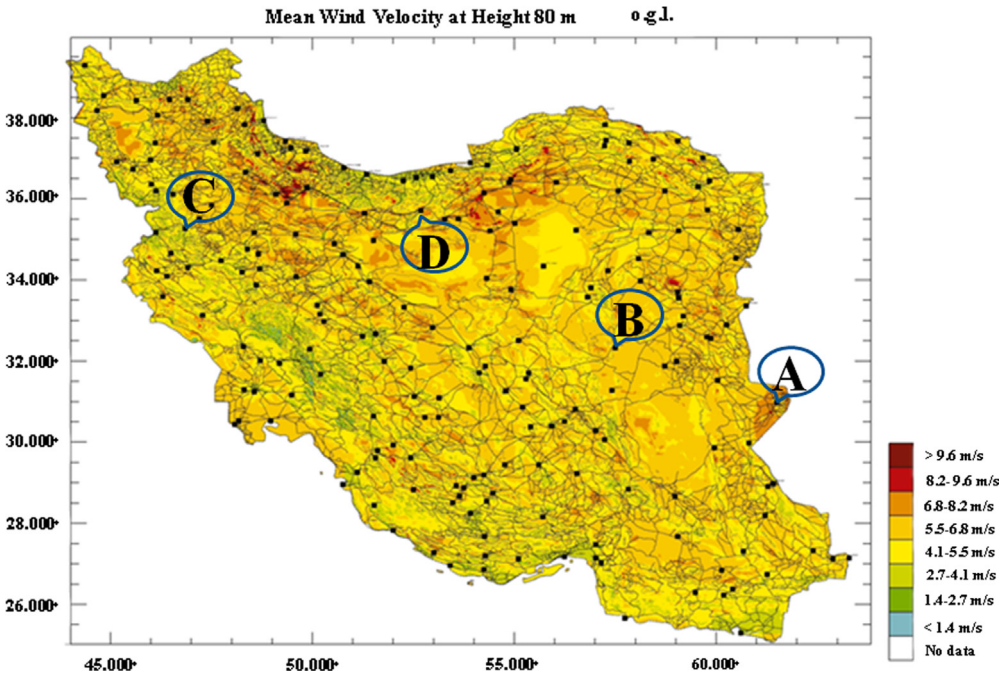

Fig. 2. Map of mean wind velocity at height 80 m in Iran with the location of the considered regions (Renewable Energy Organization of Iran).

4. Starting time modeling

During most of the starting time, the blade angular velocity increases gradually and the initially very high angles of attack of the blades reduce slowly. It is assumed that the wind does not slow down as it passes through the rotor. Using the "generic" flat-plate expressions for the lift and the drag coefficients at high angles of attack, Equation (6.17) of Wood (2011), gives the aerodynamic torque acting on the starting blade as

$$Q = N\rho U^2 R^3 \int_{r_h}^{1} (1+\lambda_r^2)^{1/2} cr \sin\theta_p (\cos\theta_p - \lambda_r \sin\theta_p) dr \qquad (4.1)$$

where r_h is the hub radius and all lengths are normalized by R and all velocities by U. Eq. (4.1) is independent of Re, on the basis of the limited evidence available for lift and drag at high angles of attack, (Wood, 2011). Thus the only effect of altitude comes through the density. The torque is assumed to accelerate the rotor, rather than produce power. Including the resistive torque of the drive-train and generator, Q_r, the equation for λ at any time during starting is

$$\frac{d\lambda}{dt} = \frac{R(Q-Q_r)}{JU} \qquad (4.2)$$

where J is the rotor inertia, which dominates the inertia of the generator and any other components, (Wood, 2011). The Ordinary Differential Equation (ODE) of (4.2) can be solved using many methods but because of the large number of calculation during the optimization procedure, the standard Adams–Moulton method was used to reduce the computational time (Wood, 2011). Eq. (4.2) was solved until tip speed ratio of the blade approaches to a user-specified λ_f set to 1 in the present study. This point defines the starting time, t_s, which is to be minimized. In other words, it is assumed that the power extraction would begin shortly after the rotational velocity of the blade tips equals the wind velocity.

A uniform density (ρ_b) was assumed in determining the rotor inertia and the attachment between the blade and rotor was neglected. Since the inertia depends on the geometry of the blade, the changes of the optimization variables (chord and twist) along the blade have a multiple effect on starting (Wood, 2011).

5. Genetic algorithm for optimization (GA)

Holland (1975) introduced GAs as an evolutionary optimization method based on a model of natural evolution. GAs use only the value of the objective function; no extra information about the objective function, such as its gradients, is required. The algorithm starts by assigning the genetic information to the initial population. This information comprises, in our case, the chord and twist. After the evaluation of the objective function for all the blades, the best of them, determined by the selection rate, are kept as parents to produce new children and the remainder discarded. In other words, the selection rate is the fraction of the population (or the blades) that should survive for the next step of the algorithm. After that, the crossover operator is applied to produce new offspring from parents. Crossover is the method of mixing the parental genetic material in forming the children. Uniform crossover, used in the present study, is preferable to the conventional types of crossover, single/two point crossover, because the children are more likely to cover the solution space effectively (Haupt and Haupt, 2004). The mutation operator provides variability in the inherited material and hopefully prevents the algorithm from converging to any local minimum. Moreover, it forces the algorithm to explore and search the solution space. Here, a linear adaptive mutation was used. In order to keep the children produced by the uniform crossover from changing, the mutation rate was set zero in the early generations of the algorithm but as the algorithm progresses, it increases linearly. Finally, the elitism operator is used to keep the best blades in each generation and prevent the GA operators from changing them (Haupt and Haupt, 2004).

5.1. Objective function

In order to maximize the output power and minimize the starting time, the objective function is defined as

$$\text{Objective function} = w\frac{C_p}{\max(C_p)} + (1-w)\frac{\min(t_s)}{t_s} \qquad (5.1)$$

Table 2
GA parameters and considered values.

Parameter	Population	Selection rate	Crossover type	Mutation rate
Value	2000, 3000	0.5	Uniform	Adaptive

Table 3
Initial input parameters for the blade optimization (Wood, 2011).

Parameter and value	Parameter and value	Parameter and value
$U_{starting}=5$ m/s	$U_{power}=10$ m/s	$Q_r=0$, 0.5 N m
$\lambda_f=1$	$\lambda_p=6.1$	Generator inertia$=0.006$ kg m^2
$R=1.06$ m	$r_h=0.125$ m	$N=3$
Minimum $c/R=0.01$	Maximum $c/R=0.2$	$\rho_b=550$ kg m^{-3}
Minimum $\theta_p=-5^\circ$	Maximum $\theta_p=25^\circ$	Maximum power$=754$ W

where w, such that $0 \le w \le 1$, is the weighting coefficient which determines the contribution of each goal in the objective function: the power to be maximized and the starting time to be minimized. It is expected that higher values of w will lead to high output power while lower values result in low starting time. The *max* and *min* values in the objective function are the maximum and minimum values from the current population. Four blades from the current generation always pass unchanged to the next generation. Two of them have the maximum values of the objective function and the two others are the blades for which the power coefficient and the starting time are maximum and minimum respectively. Table 2 lists the parameters for running the GA. The smaller population was used for the first optimization which has two design variables, i.e. chord and twist and the larger for the second optimization in which λ was added. In other words, the increase of the population size in the second optimization is due to increase in number of the design variables. The selection rate is a common value used in GA. The combination of the uniform crossover and the adaptive mutation was utilized to prompt the algorithm to explore the solution space effectively.

6. Results

The input parameters for the blade optimization are given in Table 3. The present small wind turbine is similar to that was investigated by Wood (2011). The SG6043 airfoil which was discussed earlier was also used in both studies. The operating tip speed ratio of the turbine is $\lambda_p=6.1$ and the selected permanent magnet generator had a rated power of 754 W at 550 rpm (Wood, 2011). For later discussion, note that the assumed value of $Q_r=0.5$ N m is typical of generators of this rating and the case of $Q_r=0$ will be studied for comparison, (Wood, 2011). While the constraint on the chord is typical of the limits on the manufacturing process, the maximum twist was set to avoid large changes in curvature in the transition section between the aerodynamic portion of the blade and the hub attachment. Machinability limits also set the minimum chord and twist (Clifton-Smith and Wood, 2007; Wood, 2004). Fifteen blade elements were chosen along the blade and because of large number of evaluations of the objective function, parallel processing was used to reduce the computational time. Three optimizations were performed as follows:

(a) **Basic Design:** A blade was optimized to operate at sea level and then its performance was evaluated at the four altitudes given in Table 1 using the parameters in Table 3.
(b) **Blade Redesign-1:** In order to improve the performance of the blade for each altitude, the blade was redesigned for the density and viscosity of each altitude to obtain new distributions of the chord and twist, again using the parameters in Table 3.
(c) **Blade Redesign-2:** The tip speed ratio (λ) was added as another variable and then the optimization procedure was repeated. No changes were made to the other parameters in Table 3.

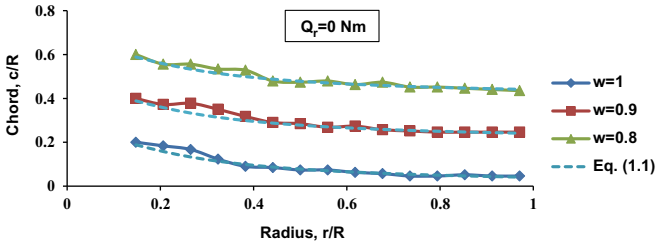

Fig. 3. Chord distributions for various weighting factors at sea level (successive plots are displaced upwards by 0.2.).

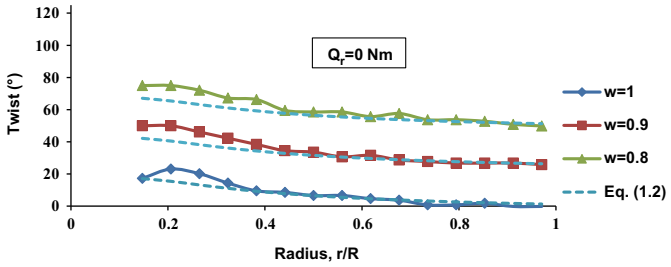

Fig. 4. Twist distributions for various weighting factors at sea level (successive plots are displaced upwards by 25°).

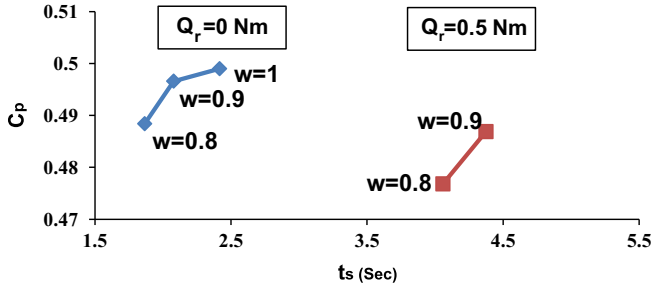

Fig. 5. The optimal front for the optimized blade at sea level.

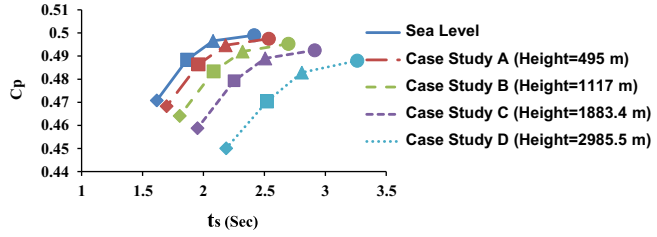

Fig. 6. The evaluation of the performance of the optimized blade at sea level in other locations, $Q_r=0$ N m (◆ $w=0.7$, ■ $w=0.8$, ▲ $w=0.9$ ● $w=1$).

6.1. Comparison of the results

In order to evaluate the accuracy of the optimization procedure, the distributions of the chord and twist have been compared with Eqs. (1.1) and (1.2) in Figs. 3 and 4 respectively. There are noticeable differences in the root region between the best blade determined by the algorithm when $w=1$ and the BEM optimum

Table 4
The average reduction of power coefficient and the average increase of starting time respect to the sea level.

Case study	A (Height=495 m)		B (Height=1117 m)		C (Height=1883.4 m)		D (Height=2985.5 m)	
	$\downarrow C_p$ (%)	$\uparrow t_s$ (%)	$\downarrow C_p$ (%)	$\uparrow t_s$ (%)	$\downarrow C_p$ (%)	$\uparrow t_s$ (%)	$\downarrow C_p$ (%)	$\uparrow t_s$ (%)
Q_r=0 N m	0.31	4.96	0.74	11.63	1.31	20.56	2.2	35
Q_r=0.5 N m	0.38	11	0.93	27.90	1.75	55.62	3.43	119.15

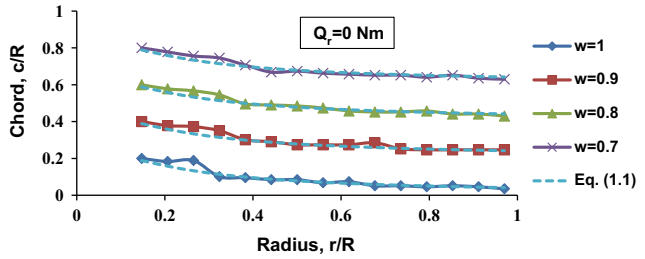

Fig. 7. Blade Redesign 1, chord distributions for case study "D" (successive plots are displaced upwards by 0.2.).

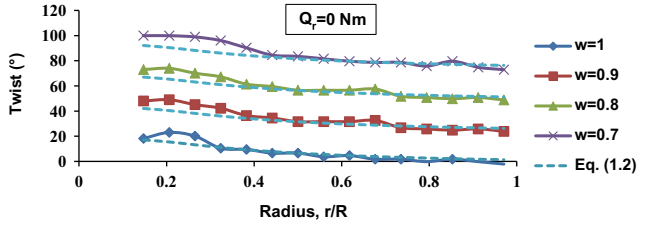

Fig. 8. Blade Redesign 1, twist distributions for case study "D" (successive plots are displaced upwards by 25°).

one as given by Eqs. (1.1) and (1.2). The present distributions for the chord and twist of the faster starting blades highlight that the improvement in the starting is mainly due to the changes in the chord and twist near the root. Fig. 5 shows the optimal fitness (Pareto) front for the output power and the starting time. The "fitness front" or "Pareto front" is the subset of the blades for which at least one part of objective function, power coefficient or inverse of starting time, is larger than that for every other blade. As it was expected, both the power coefficient and the starting time increased with increasing w, so that the most powerful blade has the poorest starting performance. Of particular interest is the noticeable displacement of the optimal fitness front in the presence of the resistive torque (Q_r=0.5 Nm). Moreover, in that case, the BEM optimum blade (w=1) could not start.

6.2. Evaluation of the optimized blade at sea level in other locations

The optimized blade for sea level was evaluated at the four altitudes. Fig. 6 shows the power coefficient and the starting time. Furthermore, the performance of the blade at each altitude in comparison with the sea level is given in Table 4 in more detail. There is, as expected, a reduction both for the power coefficient and the starting performance. While the reduction of power coefficient, due to changes in Re, seems to be unimportant, the starting time increased remarkably. This increase becomes more important for higher altitudes especially for the highest altitude - case study "D". The increase in starting time is greater than the decrease in density (and hence aerodynamic torque) because of the effect of Q_r. The results highlight the importance of considering the altitude in blade design, for any value of Q_r, but especially when it is relatively large. The need for that goal will be addressed in the following sections.

6.3. Optimization of the blade for varying altitude

The first optimization for each altitude, namely Blade Redesign-1 used the air properties listed in Table 1. For Blade Redesign-2, λ was an extra variable to be optimized rather than assigned beforehand. For a randomly selected λ in Blade Redesign-2, the power coefficient and the starting time were calculated for distributions of the chord and twist which were selected randomly as well. The procedure was continued and evolved using the GA until the value of the objective function was maximized and λ, chord and twist converged. It should be noted that the varying λ is limited in application because blades usually have to be designed to suit a particular generator and not the other way around. In other words, the choice of generator usually fixes the operating tip speed ratio (Wood, 2011).

6.3.1. Blade Redesign-1, determination of the chord and twist distribution

Figs. 7 and 8 show the distributions of the chord and twist for case study "D" – the highest altitude – for various weighting factors. The distributions of the chord and twist by Eqs. (1.1) and (1.2) are also shown in the figures. While the GA distributions are similar to BEM optimum near the tip, there is a major difference at the root sections due to the increasing importance of the starting time. Larger values of the chord and twist near the root facilitate the starting of the blade. The values of the C_P and t_s are given in Table 5. In the presence of resistive torque, the BEM optimum blade (w=1) could not start at a wind speed of 5 m/s for all case studies and more importantly, the algorithm could not find an optimal blade for case "D" for all weighting factors which is definitely due to reduction of the air density and the torque acting on the rotor. However, it should be possible to find an optimal blade for that case study as well as other cases by considering the tip speed ratio as another design variable in the optimization process which will be discussed in the next section.

6.3.2. Blade Redesign-2, determination of the chord, twist and tip speed ratio

λ was allowed to vary from 5 to 10 in addition to the other variables. Figs. 9 and 10 show the distributions of the chord and twist for case study "D" for various weighting factors. The parameters of the optimized blade for each case study are reported in Table 6. The tip speed ratio was increased in increments of 0.16 due to the binary GA parameters. In this study, the variables space was divided to 32 (2^5) bins for the chord, twist and λ. Since the range of λ was 5–10, the increment is 5/32∼0.16. Note that for w=1, the value of C_p for each altitude should be independent of Q_r. The biggest difference in the computations is in the third significant figure. Contrary to the first optimization phase, the values of C_p in Table 6 show a significant increase for almost all case studies that reveals the major issue that λ plays an important role in maximizing energy extraction. Most importantly, considering the resistive torque in the optimization process led to a significant increase in the starting time which highlights the effect of resistive torque on the starting of small wind turbines. Furthermore, the

Table 5
Blade Redesign-1, values of power coefficient and starting time for four case studies.

Case study	A (H=495 m)		B (H=1117 m)		C (H=1883.4 m)		D (H=2985.5 m)	
w	C_p	t_s (s)	C_p	t_s (s)	C_p	t_s (s)	C_p	t_s (s)
Q_r=0 N m								
1	0.4973	2.75	0.4951	2.88	0.4918	3	0.4892	3.58
0.9	0.496	2.29	0.4925	2.37	0.4892	2.76	0.4868	3.09
0.8	0.4905	2.04	0.4877	2.14	0.486	2.38	0.4808	2.73
0.7	0.4802	1.83	0.4746	1.92	0.4747	2.12	0.4651	2.34
Q_r=0.5 N m								
1	–	–	–	–	–	–	–	–
0.9	0.4914	6.52	0.4882	7.77	0.4859	10.72	–	–
0.8	0.4873	5.93	0.4846	6.14	0.4806	8.55	–	–
0.7	0.48	5.45	0.4818	5.81	0.4748	6.61	–	–

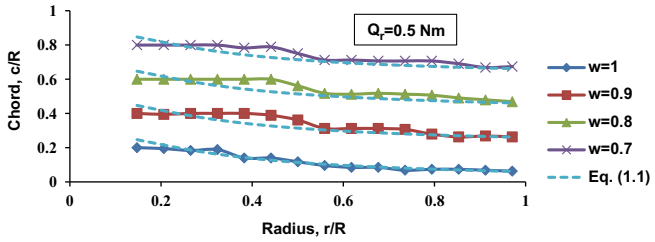

Fig. 9. Blade Redesign 2, chord distributions for case study "D" (successive plots are displaced upwards by 0.2).

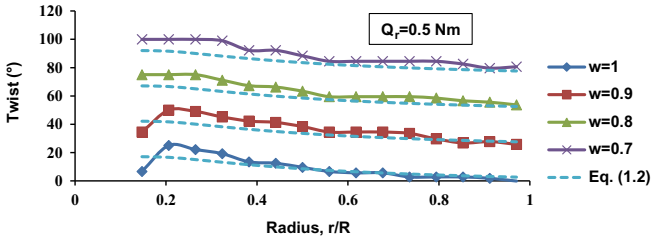

Fig. 10. Blade Redesign 2, twist distributions for case study "D" (successive plots are displaced upwards by 25°).

starting time for BEM optimum blade is larger in comparison with other weighting factors. These findings are consistent with that of previous research which emphasized that the BEM optimum blade usually has a poor starting performance.

It can be seen that the distributions of the chord and twist are not smooth especially at the root section of the blade, Figs. 7–10. The scatter becomes larger for the higher weighting factor, and as w reduces, the distributions become smoother. Since the root section of the blade contributes little to the power production, the genetic algorithm is not forced to find the smooth distributions at the inner sections of the blade for the higher values of w. On the other hand, for lower values of w, the contribution of the starting becomes more important in the objective function and the algorithm is forced to find smoother distributions for the chord and twist for the root sections. Obviously, the scattered results for the twist and chord that arise from numerical optimization cannot be used for blade design. Wood (2004) found that fitting third or fourth order least squares polynomials to the scattered results provided smooth chord and twist distributions which the starting time and the power performance of the new blades were very similar to the scattered ones.

7. Discussion

In order to investigate the effect of the two optimization phases, the optimal front for two case studies is shown in Figs. 11 and 12. The effect of the resistive torque will be discussed in more detail in the next section. In both the optimization phases, an improvement was achieved with respect to the initial blade which was designed for sea level. Generally, an increase is seen both for the power coefficient and the starting time in the optimal front in Fig. 11. It is seen that the variations of the power coefficient with altitude are not significant in those figures. This constancy of the power coefficient occurs due to the relatively small values of Reynolds number over the blade sections which change the lift to drag ratio of the blade sections. The changes of Re is mainly due to the change in the kinematic viscosity (ν) which increases as the altitude increases. The values of the kinematic viscosity, average Re over the whole blade and the corresponding power coefficient for all case studies as well as sea level case are provided in Table 7 for Blade Redesign-1. The changes of the kinematic viscosity and average Re respect to the sea level are also provided in Table 7. Results show that the decrease in Re, obtained by the present study, is similar to increase of kinematic viscosity which was obtained according to the ISA (U.S. Standard Atmosphere, 1962). However, the reduction of Re is not very pronounced and it would not cause a major decrease in the aerodynamic coefficients which determine the torque and the power. So, the decrease of the power coefficient in Blade Redesign-1 is not large especially for the lower altitudes. It should be noted that although the power coefficient remains approximately constant, the output power would naturally decrease with the increase of altitude due to the reduction of the air density.

While the variations of the power coefficient are small, the changes of the starting time are more evident in Figs. 11 and 12. According to Eq. (4.1), the torque acting on the blade is proportional to the ρ with no variation with Re. Since the air density reduces as the altitude increases, the torque acting on the blade decreases as well. Moreover, the aerodynamic torque is small at low wind speed and so any decrease in it has a greater than the proportionate effect on net starting torque. So, it can be deduced that the increase of the starting time at high altitudes is unavoidable. However, it could be possible to take some measures to reduce the starting time. The easiest way is to reduce w to put more weight on the starting in the objective function. Another way is to use less dense blade material to lower the rotor inertia of the blade and the idling period. The lower value of the blade density is very desirable not only for the starting time but also for the mass minimization of the blade. Nevertheless, in that case the cost and structural issues of the blade should be also

Table 6
Blade Redesign-2, the tip speed ratio with corresponding power coefficient and starting time.

Case study	A (H=495 m)			B (H=1117 m)			C (H=1883.4 m)			D (H=2985.5 m)		
w	C_p	t_s	λ	C_p	t_s	λ	C_p	t_s	λ	C_p	t_s	λ
Q_r=0 N m												
1	0.4986	3.08	5	0.4982	3.18	5.16	0.4967	3.49	5.16	0.4933	4.06	5
0.9	0.4981	2.80	5.16	0.4964	2.61	5.48	0.4931	3	5.32	0.4921	3.71	5.16
0.8	0.4913	2.31	5.48	0.4894	2.33	5.48	0.491	2.92	5.48	0.4861	3.02	5.48
0.7	0.4855	2.1	5.48	0.4804	2.15	5.48	0.478	2.36	5.48	0.4686	2.57	5.81
Q_r=0.5 N m												
1	0.4988	8.45	5.16	0.4973	9.04	5	0.4963	13.53	5.16	0.4935	29.24	5
0.9	0.4963	5.11	5.32	0.4924	5.45	5	0.4915	6.54	5.16	0.4888	8.51	5.16
0.8	0.4902	4.75	5.16	0.4896	5.12	5.16	0.4817	5.62	5	0.4776	6.83	5
0.7	0.4761	3.93	5	0.4726	4.42	5	0.473	4.99	5	0.4705	6.35	5

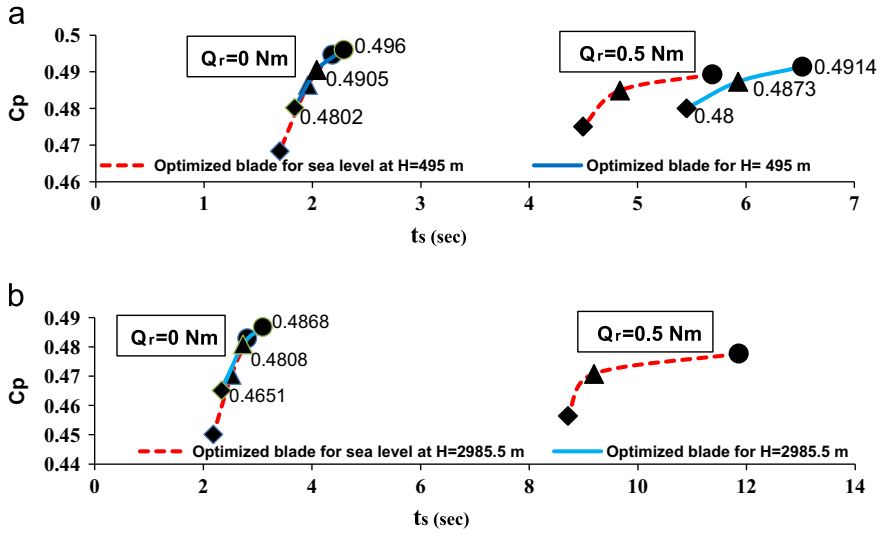

Fig. 11. The optimal fitness front for two case studies, Blade Redesign-1, (◆ w=0.7 ▲ w=0.8, and ● w=0.9). (a) Case Study A (H= 495 m) and (b) Case Study D (H= 2985.5 m).

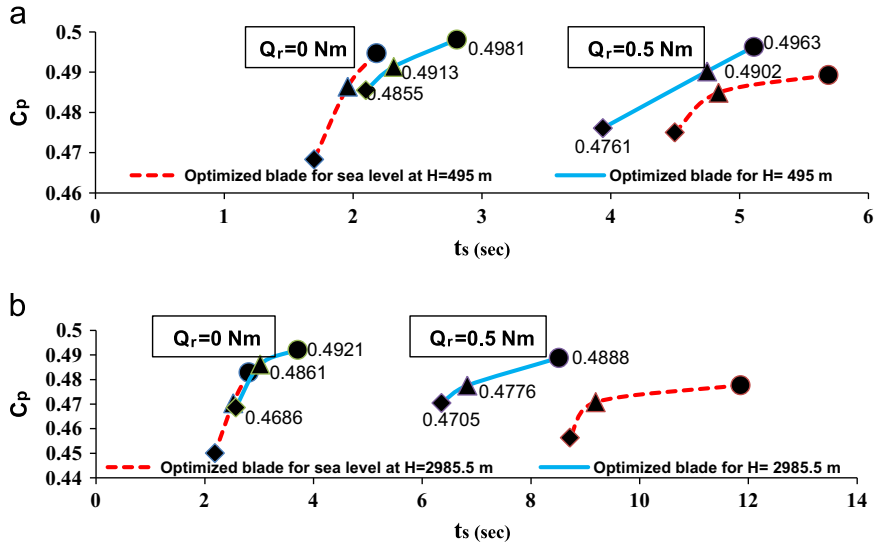

Fig. 12. The optimal fitness front for two case studies, Blade Redesign-2, (◆ w=0.7, ▲ w=0.8, and ● w=0.9). (a) Case Study A (H= 495 m) and (b) Case Study D (H= 2985.5 m).

considered thoroughly during the turbine design. An increase in N could also reduce the starting time. However, it is worth noting that in the absence of resistive torque (Q_r=0), Eq. (4.2) implies that the starting time is independent of the number of blades because the rotor inertia, like Q, is linear in N.

7.1. The effect of resistive torque

The results discussed in the previous sections show that the resistive torque plays an important role in design and optimization of small wind turbine blades. When Q_r=0.5 N m was added to

Table 7
Blade Redesign-1, variations of kinematic viscosity (ν), average Reynolds number (Re) over the whole blade and the power coefficient (C_p), Q_r=0 Nm.

Case study	Height (m)	C_p	ν (m^2/s) (ISA)	$\uparrow\nu$ (%)	Average Re	$\downarrow Re$ (%)
Sea level	0	0.499	1.46E-05	–	1.85E05	–
A	495	0.4973	1.52E-05	3.98	1.77E05	4.64
B	1117	0.4951	1.60E-05	9.28	1.66E05	10.28
C	1883.4	0.4918	1.70E-05	16.28	1.52E05	17.83
D	2985.5	0.4892	1.86E-05	27.39	1.37E05	25.94

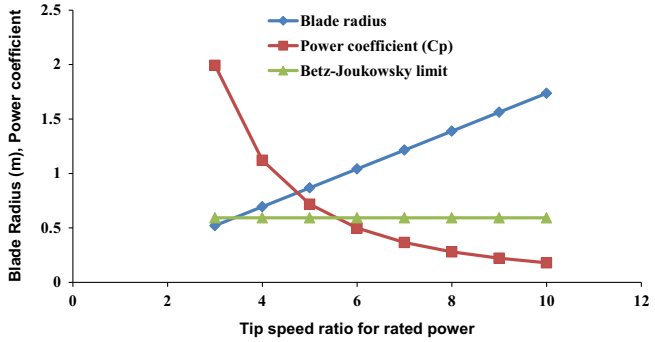

Fig. 13. Variation in power coefficient and blade radius with tip speed ratio for rated power.

Eq. (4.2), the optimal fitness front dramatically changed and t_s was significantly increased (Figs. 11 and 12). As shown in Figs. 11 and 12, C_p for Q_r=0 is generally larger than for Q_r=0.5 N m. In order to overcome the resistive torque, the algorithm found a blade with larger chord and twist in the hub section than the optimal power extracting blade, which decreased C_P.

Contrary to the Blade Redesign-1 where only the power coefficient increased, the results showed that in the Blade Redesign-2 for Q_r=0.5 N m, both C_P and t_s improved over the optimized blade working at the sea level (Fig. 12). These improvements are because of considering the tip speed ratio as an extra variable which freed the algorithm to find blades to meet the objective function goals. So, in the second optimization procedure and for Q_r=0.5 N m, C_P was slightly increased and t_s decreased especially for the higher altitudes (Fig. 12).

The increase in t_s becomes more important as the altitude increases. The results for case "D" show that for Q_r=0.5 N m the first re-design could not find an optimal blade for that altitude that would start at 5 m/s. When the generator characteristics do not change with altitude, the results indicate that in the very high altitudes, a change in starting performance is inevitable. However, the only way that resistive torque could change with altitude is if the generator had a gearbox where lubrication friction was important in which case it is likely that Q_r would increase with altitude. Considering λ as another variable in the Blade Redesign-2, new blades were found for case "D", Table 6 and Fig. 12. However, as it was mentioned earlier, in that case the characteristics of the electrical generator must be changed. It should be noted that with the fixed generator, it is possible to vary the length of the blade to reduce the starting time if this does not change the blade cost too much (Wood, 2011).

7.2. Determination of the appropriate weighting factor

It is the nature of multi-dimensional optimization that a single optimal design is rarely achieved. Instead, the Pareto fronts as shown above, give the locus of optimum blades for two-dimensional optimization. The remaining question is to determine the appropriate value of w for the final design; alternatively, deciding which point along the Pareto front constitutes the final "optimal" design. This is done by following the design example in Wood, (2011) where the blades were designed for a 754 W generator at the rated rotational speed of 550 rpm with efficiency, η, of 74%. Assuming a rated wind speed of 10 m/s gives the following equations for C_P, and λ_p:

$$C_P = \frac{P/\eta}{(1/2)\rho A U^3} = \frac{754/0.74}{(1/2)\times 1.2\times 10^3\times \pi R^2} = 0.541/R^2 \quad (7.1)$$

$$\lambda_P = \frac{R\Omega}{U} = \frac{550\times 2\pi}{10\times 60} R = 5.795R \quad (7.2)$$

Variations in C_p and R with λ_p are shown in Fig. 13 together with Betz-Joukowsky limit (16/27∼0.6). For any value of R, C_p could be found by Eq. (7.1) but C_P>16/27 is infeasible. The largest practical C_P that can be achieved is a matter of judgment, but the authors are unaware of any SWT with C_P>0.48, approximately. Choosing R=1.06 m gives C_p=0.481 and λ_p=6.10 which was used in Blade Redesign-1 (Table 3). In other words, the blade radius and the tip speed ratio are selected to match the power and the rotational speed of the chosen generator. Regarding Fig. 5, for Q_r=0.5 N m, w=0.9 is an appropriate weighting factor, but for Q_r=0 N m, both w=0.8, 0.9 could be selected but a blade with w=0.8 obviously have a better starting performance. It should be noted that the w>0.7 are usually selected for multi-dimensional analysis because for lower values of w, the importance of the power, the main goal of the wind turbine blade design, drops in the objective function and BEM analysis could not find a reasonable distribution for the chord and twist.

8. Conclusions

In this study, the effect of the air density variation with altitude on the performance of a small wind turbine blade was investigated. Four regions in Iran with different altitudes were selected and the multi-dimensional blade design and optimization was undertaken assuming that the air density and viscosity varied according to the International Standard Atmosphere (U.S. Standard Atmosphere, 1962). A genetic algorithm was specifically written for the optimization which combined power extraction with starting time and included typical values of generator resistive torque. The performance of a blade designed for operating at sea level degraded at higher altitudes. The reduction in the power coefficient was largely due to the decrease in air density but the much larger degradation in starting was due to the increasing importance of the resistive torque which was assumed to be independent of altitude. The density changes are the nearly the same for starting torque as for power production torque. However, the former is smaller by at least and order of magnitude, and so is greatly affected by subtracting a constant resistive torque. So, an increase in the starting time for the small wind turbines which are operated at high altitudes is unavoidable. However, it is possible to improve the blade performance for those altitudes. Two approaches were carried out to address that goal. At the first attempt, the geometry of the blade, in terms of chord and twist, was optimized for the appropriate air density that increased both the power coefficient and the starting time. Using the second approach, much more power was achieved by adding the tip speed ratio to the other variables (chord and twist) in the optimization process. In the both approaches, including the resistive torque in the optimization process led to a noticeable change in the optimal fitness front. The inclusion of the resistive torque was more important especially for the higher altitudes in which the starting time was remarkably larger than lower ones and in some cases the

blade could not start with the same electrical generator working at the sea level.

Acknowledgments

DHW's involvement in this work was supported by the Canadian National Science and Engineering Research Council under their Industrial Research Chairs Program in conjunction with the ENMAX Corporation.

References

Burton, T., Sharpe, D., Jenkins, N., Bossanyi, E., 2011. Wind Energy Handbook, 2nd edition John Wiley and Sons, United Kingdom, http://dx.doi.org/10.1002/9781119992714.

Clifton-Smith, M.J., Wood, D.H., 2007. Further dual purpose evolutionary optimization of small wind turbine blades. J. Phys.: Conf. Ser., 75, http://dx.doi.org/10.1088/1742–6596/75/1/012017.

Clifton-Smith, M., 2009. Wind turbine blade optimisation with tip loss correction. Wind Eng. 33, 477–496, http://dx.doi.org/10.1260/030952409790291226.

Clifton-Smith, M., 2010. Aerodynamic noise reduction for small wind turbine rotors. Wind. Eng. 34, 403–420, http://dx.doi.org/10.1260/0309-524X.3.4.403.

Ebert, P.R., Wood, D.H., 1997. Observations of the starting behaviour of a small horizontal-axis wind turbine. Renew. Energy 12 (3), 245–257, http://dx.doi.org/10.1016/S0960-1481(97)00035-9.

Giguere, P., Selig, M., 1998. New airfoils for small horizontal axis wind turbines. J. Sol. Energy. Eng. 120, 108–114, http://dx.doi.org/10.1115/1.2888052.

Holland, J.H., 1975. Adaptation in Natural and Artificial Systems. University of Michigan Press, Ann Arbor

Hampsey, M., 2002. Multiobjective Evolutionary Optimisation of Small Wind Turbine Blades (PhD thesis), University of Newcastle.

Haupt, R.L., Haupt, S.E., 2004. Practical Genetic Algorithms, second ed. John Wiley and Sons, New York.

IEC, 2006. IEC 61400-2. Wind Turbines. Part 2 – Design Requirements for Small Turbines, 2nd ed. March 2006.

Keyhani, A., Ghasemi Varnamkhasti, M., Khanali, M., Abbaszadeh, R., 2010. An assessment of wind energy potential as a power generation source in the capital of Iran. Tehran Energy 35, 188–201, http://dx.doi.org/10.1016/j.energy.2009.09.009.

Mayer, C., Bechly, M., Hampsey, M., Wood, D.H., 2001. The starting behaviour of a small horizontal-axis wind turbine. Renew. Energy 22, 411–417, http://dx.doi.org/10.1016/j.jweia.2004.08.003.

Mostafaeipour, A., Abarghooei, H., 2008. Harnessing wind energy at Manjil area located in north of Iran. J. Renew. Sustain. Energy Rev. 12, 1758–1766, http://dx.doi.org/10.1016/j.rser.2007.01.029.

Mostafaeipour, A., 2010. Feasibility study of offshore wind turbine installation in Iran compared with the world. J. Renew. Sustain. Energy Rev. 14, 1722–1743, http://dx.doi.org/10.1016/j.rser.2010.03.032.

Mostafaeipour, A., Sedaghat, A., Dehghan-Niri, A.A., Kalantar, V., 2011. Wind energy feasibility study for city of Shahrbabak in Iran. J. Renew. Sustain. Energy 15, 2545–2556, http://dx.doi.org/10.1016/j.rser.2011.02.030.

Mostafaeipour, A., Jadidi, M., Mohammadi, K., Sedaghat, A., 2014. An analysis of wind energy potential and economic evaluation in Zahedan, Iran. J. Renew. Sustain. Energy. Rev 30, 641–650, http://dx.doi.org/10.1016/j.rser.2013.11.016.

U.S. Standard Atmosphere, 1962, U.S. Government Printing Office, Washington, D.C.

Wright, AD., Wood, D.H., 2004. The starting and low wind speed behaviour of a small horizontal axis wind turbine. J. Wind Eng. Ind. Aerodyn. 92, 1265–1279, http://dx.doi.org/10.1016/j.jweia.2004.08.003.

Wood, D.H., 2004. Dual purpose design of small wind turbine blades. Wind Energy 28 (5), 511–527, http://dx.doi.org/10.1260/0309524043028037.

Wood, D.H., Robotham, T., 1999. Design and testing of high performance blades for a 600 W horizontal axis wind turbine. In: Proceedings of the first Australian Wind Energy Conference, Newcastle, June 28–30, pp. 91–96.

Wood, D.H., 2011. Small Wind Turbines: Analysis, Design, and Application, Green Energy and Technology. Springer, UK, http://dx.doi.org/10.1007/978-1-84996-175-2.